

## LIA LONGITUDINAL COUPLING IMPEDANCE

Andris Faltens  
Lawrence Berkeley Laboratory

The beam generated fields enter into the problems of waveform generation and longitudinal stability. In the former, provision must be made for the longitudinally defocusing forces due to the space charge and the beam loading effects on the accelerating voltage due to the current of a presumably known bunch. In the latter, the concern is for the growth of unintentional perturbations to unacceptably large values through the interaction of the charge and current fluctuations with the rest of the beam and the surrounding structures. These beam generated electric fields may be related to the beam current through a coupling impedance,  $Z' = \frac{E_z}{I}$ .

The problem of longitudinal stability and its dependence on the coupling impedance is well known in the design of proton storage rings and other circular machines, where it often limits attainable intensities; some of the theory and formalism may be applied to linear machines, with suitable modifications. For circular machines the usual definition has been

$$Z_n = \frac{V_n}{I_n} = \frac{2\pi R E_n}{I_n},$$

where  $E_n$  is the peak azimuthal electric field generated by a sinusoidally modulated current,  $I_n$ , of the spatial harmonic number  $n$  in a machine of radius  $R$ . The theory of space charge waves as developed for microwave tubes is analogous, though less known in the accelerator community, and uses an interaction or Pierce impedance which relates the longitudinal electric field in the region of the beam to the average power flow through an external circuit,

$$Z_p = \frac{E_z 2\lambda^2}{8\pi^2 P_{av}}$$

for a beam wavelength,  $\lambda$ , and a wall impedance

$$Z_w = \frac{E_z}{H_\theta} \Big|_{\text{wall}},$$

which is useful for matching fields at a wall boundary. Both of the microwave tube impedances emphasize the surrounding structure, while the accelerator coupling impedance combines the effects of space charge and external structure.

For the purposes of a high current linear accelerator it appears useful to maintain some distinction between the space charge fields and the fields due to the interaction of the beam current with structure, and to define

$$Z'(\omega) = Z'_q(\omega) + Z'_{\text{ext}}(\omega) = \frac{E(\omega)}{I(\omega)},$$

where the subscript  $q$  refers to the space charge

contribution, and the subscript ext refers to the external structure.  $Z'(\omega)$  is the ratio of the electric field to the beam current amplitudes for a sinusoidally modulated current at angular frequency  $\omega$ , has the dimensions of ohms per meter, and in general is complex because the electric field is usually phase shifted with respect to the current. No special emphasis is given to any particular set of harmonics in the LIA because a single bunch is accelerated in a non-steady-state manner.

 $Z_q$ 

The self-fields are within a factor of  $1-\beta^2$  the electrostatic fields of the modulated charge, and may be calculated by transforming the electrostatic fields of a stationary charge distribution to a moving coordinate frame. For the HIF applications  $\beta^2 \ll 1$  because of the low particle speed,  $\beta c$ . For modulation wavelengths long compared to the chamber radius,  $b$ , a beam of radius  $a$  has

$$Z'_q(\omega) = j\omega^2(-L)'' \approx \frac{j\omega\mu_0}{2\pi\beta^2} \left( \ln \frac{b}{a} + \frac{1}{2} \right),$$

where the factor,  $\ln \frac{b}{a} + \frac{1}{2}$ , often called  $g$  for a geometry factor, applies to the particles at the center of the vacuum chamber and a factor  $\ln \frac{b}{a} + \frac{1}{4}$  is more appropriate if the average electric field over all particles is required. Insofar as this  $g$  factor is of order unity and changes slowly with the beam-chamber geometry,  $Z'_q(\omega)$ , the self-field contribution, is of the same order of magnitude at low frequencies for the induction linac, the rf linac, or the storage ring, depending mainly on the velocity of the particles. The sign of  $Z'_q$  is capacitive, that is, in the sense that the bunch would be caused to expand longitudinally, but the frequency dependence is like that of an inductor, therefore, it acts as a negative inductance, "-L". In principle, the self-impedance could be partly compensated by a positive inductive wall impedance, with inductances comparable to those in the induction acceleration cores. The compensation could only be partial because of the field variation across the beam and because of frequency dependent transit time effects.

The frequency range where the long wavelength approximation fails depends on the chamber dimensions. Physically, for short wavelengths the electric field preferentially goes from regions of greater charge density to regions of lower density within the beam, rather than to the wall as in the low frequency limit. The boundary between the long and short wavelength approximations is in the region where

$$ka \approx kb = \frac{\omega b}{v} = \frac{2\pi b}{\lambda} \approx 1, \text{ or } \omega \approx \frac{\beta c}{b}.$$

In the short wavelength limit,

$$Z'_q(\omega) = \frac{1}{j\omega''C''} \approx \frac{1}{j\omega\epsilon_0\pi a^2},$$

and it behaves as a capacitor, "C".

The maximum value of  $Z'_q$  therefore is in the region  $\omega \approx \frac{\beta c}{b}$  and has the values

$$Z'_q \text{ max} \approx -\frac{j60}{\beta b} \left(\ln \frac{b}{a} + \frac{1}{2}\right) \text{ or } \frac{-j120}{\beta a}$$

in the two limits. The lower of these, for  $(\ln \frac{b}{a} + \frac{1}{2}) \approx 1$ , gives

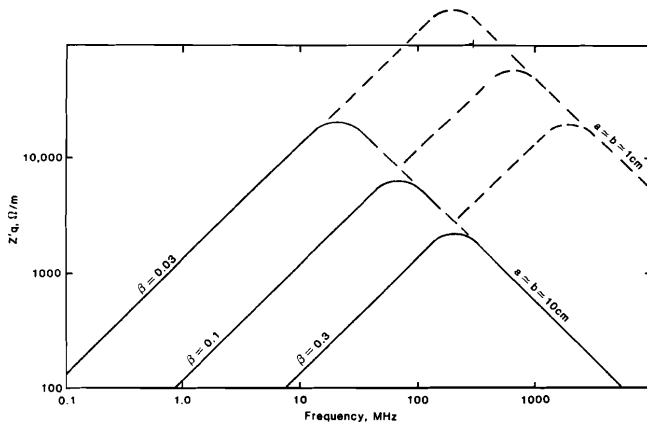
$$Z'_q \text{ max} \approx -\frac{j600}{\beta} \Omega/\text{m for } b \approx 10 \text{ cm,}$$

as would be typical in the induction linac or storage ring, and  $Z'_q \text{ max} \approx -\frac{j6000}{\beta} \Omega/\text{m}$  for  $b \approx 1 \text{ cm}$  as in a typical rf linac, with  $\omega_{\text{max}} \approx 3 \times 10^9 \beta$  and  $3 \times 10^{10} \beta$  respectively. Since  $\beta$  has a maximum value of about 1/3 for HIF, the space charge impedance peaks in the neighborhood of 100 MHz and 1000 MHz for the large and small chamber machines, respectively.

A sketch of the self-field impedance is shown in Figure 1 for a range of  $\beta$ 's and chamber radii that span the HIF range.

Z<sub>ext</sub>

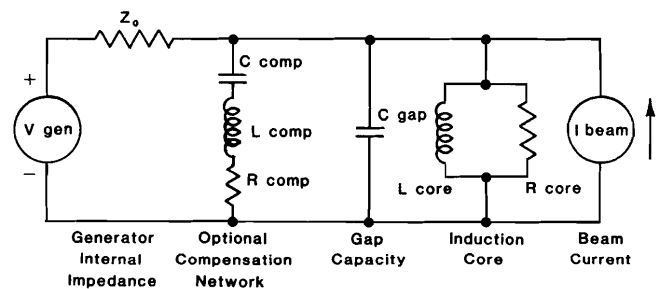
The external or wall impedance,  $Z'_{\text{ext}}$ , includes the effects of the accelerating gaps and other discontinuities in the beam line as well as a relatively unimportant contribution from the skin or surface impedance of the chamber wall itself.  $Z'_{\text{ext}}$  is easier to estimate and manipulate in an induction linac than in other accelerator structures because the LIA "cavity" is filled with rf absorbing material and is tightly coupled to a low impedance generator. By contrast, an rf cavity is a high-Q structure designed to attain an impedance of several Meg  $\Omega/\text{m}$  on resonance, and usually is loosely coupled to a generator.



The Self-field Contribution,  $Z_q$ , to the Coupling Impedance for  $\beta$  0.03, 0.1, and 0.3 and Radius 10 cm (LIA) and 1 cm (rf Linac) Figure 1

While phase and amplitude feedback may regulate the fundamental mode voltage and thereby lower the impedance seen by the beam, little seems to be known about the higher modes other than that they shouldn't be harmonically related to the fundamental of the rf. Because of these differences in the structures and coupling,  $Z'_{\text{ext}}$  in an LIA cavity is to a large extent determined by the generator which drives it, while in an rf cavity it is mainly a property of the structure itself.

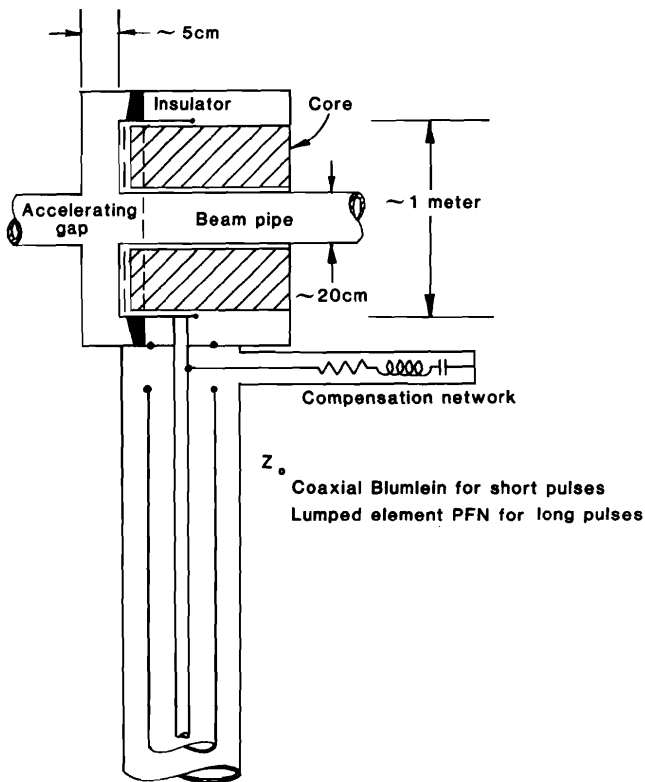
The LIA  $Z'_{\text{ext}}$  is well represented over the most important frequency range by the circuit shown in Fig. 2., which may be directly related to the induction module and drive circuit shown in Fig. 3. The generator impedance,  $Z_0$ , is the characteristic impedance of the pulse forming network or line used to drive the module, and is the dominant element for frequencies of the order of the reciprocal of the pulse duration. At higher frequencies, the generator impedance is shunted by the gap capacity,  $C_g$ , which is about two orders of magnitude higher than the usual gap capacity of an rf cavity. The induction core has a relatively minor role compared to the first two elements. Because of the non-ideal behavior of the induction core, whether it is ferrite or iron, eddy current and magnetization currents have the appearance shown in Fig. 4, for a constant applied voltage, rather than the linearly increasing and smaller current which is shown dashed in Fig. 4. The actual current response suggests an equivalent circuit for the core which consists of a parallel  $R_C$ - $L_C$  combination, with the resistive part,  $R_C$ , dominant. At very low frequencies the core does have inductive behavior. An optional compensation network, shown as the  $L_{\text{comp}}$ - $R_{\text{comp}}$ - $C_{\text{comp}}$  series string may be used for pulse shaping purposes, such as speeding up the rise time and modifying the slope of the voltage, or the same function may



- Representative values:  $L_{\text{core}} = 10^{-4} - 10^{-3} \text{ Hy}$   
 $R_{\text{core}} = 1-2 \text{ k}\Omega$   
 $C_{\text{gap}} = 100-200 \text{ pF}$   
 $Z_0 = 100-1000 \Omega$

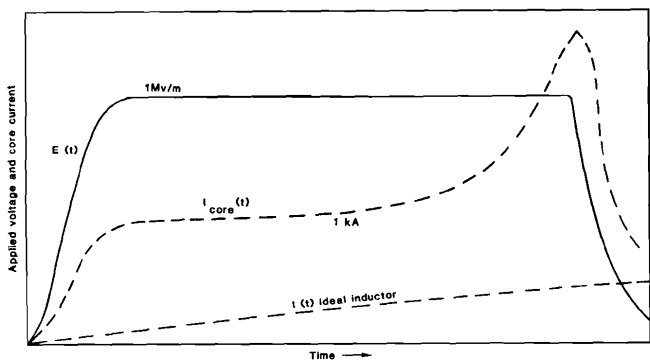
Accelerator Equivalent Circuit

Figure 2



Induction Acceleration Cavity and Voltage Generator

Figure 3



Approximate Form of Core Excitation Current

Figure 4

be obtained by tailoring the generator impedance. A desirable core has

$$R_{core}, R_{comp} \gg Z_0,$$

and

$$Z_0 \approx \frac{V_{gap}}{I_{beam}},$$

Most of the effort has been expended on decreasing the core losses, which allows  $Z_0$  to be raised.

The choice of the generator impedance,  $Z_0$ , is influenced by efficiency considerations. The voltage appearing across the accelerating gap is the sum of the applied voltage and the beam generated voltage, with the approximations that the source is a generator matched to a transmission line with a characteristic impedance,  $Z_0$ , that the gap capacity is negligible, that the core impedance is infinite, and that all components are linear.

$$V_{gap} = V_{incident} + V_{reflected} - I_{beam} R_{beam},$$

where  $R_{beam}$  is the parallel combination of  $Z_0$  and  $R_{core}$

$$R_{beam} \equiv R_b = Z_0 || R_{core},$$

and is equal to the external coupling impedance,  $Z'_{ext}$  in this approximation.

For this model, the acceleration efficiency,  $\eta$ , is

$$\eta = \left( \frac{R_{core}}{Z_0 + R_{core}} \right) \left( \frac{I_{beam} Z_0}{V_{incident}} \right) \left( 2 - \frac{I_{beam} Z_0}{V_{incident}} \right),$$

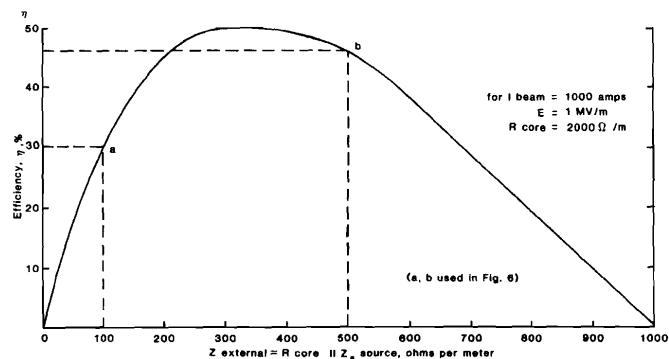
with a maximum value

$$\eta_{max} = \frac{R_{core}}{Z_0 + R_{core}},$$

which may approach 1. The efficiency in terms of the external coupling impedance is

$$\eta = \frac{4 I_b^2 Z_{ext}^2 V_{gap}}{Z_0 (V_{gap} + I_b Z_{ext})^2}.$$

$\eta$  is plotted versus  $Z_{ext}$  in Fig. 5. Near the maximum efficiency point the function is flat; therefore,  $Z_{ext}$  may be reduced by a factor of two or three without a comparable loss of efficiency. Lowering the generator impedance is



Dependence of Efficiency on the External Coupling Impedance at the Peak of the  $Z(\omega)$  Curve

Figure 5

advantageous in the short pulse region, where transmission lines are acceptable voltage sources, because it is difficult to build high voltage, high impedance lines, and because a lower impedance line allows the gap capacity to be charged faster.

At frequencies comparable to the reciprocal of the acceleration pulse rise time, the wall impedance is dominated by the gap capacity. For the gap capacity to be treated like a lumped element, the two way travel time for electromagnetic waves from the inner radius to its outer radius should be less than a quarter cycle,

$$\frac{2\Delta r}{c} < \frac{T}{4}, \text{ or equivalently } \Delta r < \frac{\lambda_{\text{free space}}}{8}.$$

where  $\Delta r$  is the difference between the outer radius,  $A$ , and the bore radius,  $b$ . A typical  $\Delta r$  is 50 cm, therefore, the lumped element approximation is satisfactory for  $f < 75$  MHz. The actual value of the gap capacity

$$C \approx \frac{\epsilon_0 \pi A^2}{d},$$

for a gap of width  $d$ , depends to a large extent on  $d$ . Within bounds,  $d$  is a free parameter, with the minimum set by voltage breakdown, and a value near 5 cm satisfactory, for which  $C \approx 140$  pF. The inclusion of the gap capacity leads to a lower value of the wall impedance;

$$Z_{\text{ext}} \rightarrow \frac{R}{1 + j\omega RC} = \frac{R}{1 + (\omega RC)^2} - \frac{j\omega R^2 C}{1 + (\omega RC)^2},$$

with the dependences

$$|Z_{\text{ext}}| \propto \frac{1}{\omega} \text{ and } \text{Re}(Z_{\text{ext}}) \propto \frac{1}{\omega^2},$$

as the frequency is increased.

Transit time function,  $T_r$

In the frequency region where the gap capacity becomes important and above, the effects due to the change in the electric field during the transit of the particles through it becomes significant also, and tend to lower the external impedance by the factor  $T_r^2$ , where

$$T_r = \frac{\langle \int_{-\infty}^{\infty} E(r,z) \cos \omega t dz \rangle}{\langle \int_{-\infty}^{\infty} E(r,z) ds \rangle}$$

along the particle trajectories. In a gridded

gap with uniform fields,  $T_r = \frac{\sin \pi d / \lambda}{\pi d / \lambda}$ , and

has a null at about 600 MHz for our example, with  $\beta \approx 1/10$ . In an open geometry such as the real accelerating gap,  $T_r$  will start decreasing at lower frequencies because of the extension of the field into the bore tube, say, at 300 MHz

for the previous example. At any  $\beta$ ,  $T_r$  will also decrease when the frequency approaches the waveguide cutoff frequency of the vacuum chamber, which is  $\sim 1.1$  GHz for this example. The detailed geometry of the gap region may be adjusted rather freely to change  $T_r$  without affecting the functioning of the cavity.

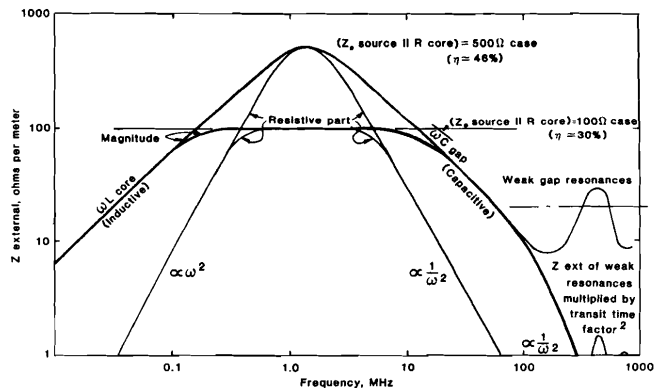
High Frequency Limit

At the highest frequencies, the accelerating gap geometry may be approximated as a radial transmission line. If the line were tapered to achieve a constant impedance, its value would be

$$Z_{\text{radial}} \approx \frac{60d}{a} \approx 30 \Omega \text{ (resistive)},$$

while in the parallel disc geometry it would be less. At the cavity outer radius, the radially outgoing radiation is well absorbed by the magnetic core material, which may be facilitated by making a gradual rather than abrupt transition into the material (e.g., ferrite). This is quite the opposite from the usual situation in an rf cavity, where the reflection of waves is essentially lossless, and results in a series of resonant peaks in the impedance at the frequencies where the reflections all add up in phase. In an induction cavity, because of the loading with rf absorbing magnetic material, only the vestiges of the usual resonant behavior remain, and these are bounded in magnitude to some tens of ohms. The impedance function is modulated by the transit time factor squared, and therefore the resonant peaks have a  $\frac{1}{\omega^2}$  dependence at high frequencies, roughly in the range between 100 and 1000 MHz.

The various ingredients of  $Z_{\text{ext}}$  and the frequency ranges where they apply are shown in Fig. 6. It should be noted that the peak of the impedance function is well below the microwave region, and that this peak is determined by the external circuitry rather than being an intrinsic property of the structure. The 500  $\Omega$  line shown is near the maximum attainable impedance for a generator matched to the beam in a cavity using available core materials; the 100  $\Omega$  line is for a mismatched source. If



The External or Wall Impedance Part of the Coupling Impedance for  $Z_{\text{source}} \text{ Source II R core} = 100 \Omega/\text{m}$  and  $500 \Omega/\text{m}$   
Figure 6

necessary, the impedance could be lowered below the values shown by modifying the external circuitry.

Applications

The coupling impedance enters into the calculation of the applied voltages and into the longitudinal stability problem. The voltage seen by the bunch is the sum of the applied voltage and the beam generated voltage: this latter is composed of two parts, which may be approximated as

$$E_{\text{beam}} = - I_{\text{beam}} R' + "L" \frac{dI_{\text{beam}}}{dt} ,$$

where  $R'$  is the resistive impedance seen by the beam and " $L$ " is a measure of the space charge forces generated by charge density gradients with the bunch. In a long bunch the charge density gradient is expected to be localized near the ends of the bunch. When the applied and beam generated forces are added together, the field seen by any particle is constant anywhere within the bunch. A small additional field is required at the tail of the bunch to reflect off-momentum particles and create the equivalent of a synchrotron bucket, with the major difference that the applied voltages are not constrained to be sinusoidal. These major components are shown in Fig. 7. One of the areas of active investigation at LBL is the sensitivity of the bunch to errors in the applied waveforms, and the growth of the longitudinal emittance by "noise" in the

acceleration process. On a single particle basis, as would apply to a particle in the middle of the bunch, most of the voltage errors, if random, are expected to average out, and the

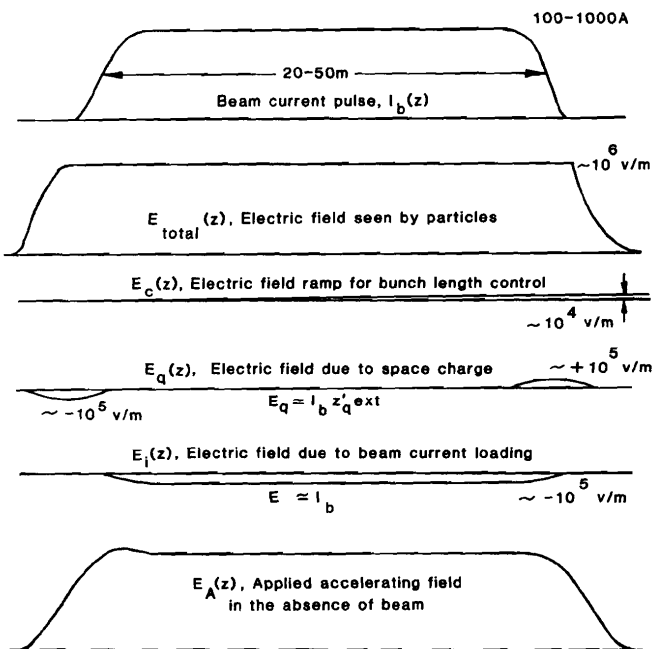
energy spread should grow as  $\frac{\Delta E}{E} \approx \frac{1}{\sqrt{n}} \left( \frac{\Delta V}{V} \right)$  where  $n$  is the number of acceleration gaps, about  $10^4$ , and  $\Delta V/V$  is the fractional voltage error per gap.

The longitudinal stability of the beam against small perturbations depends on the detailed nature of the coupling impedance, the form of the particle distribution function, and the square of the velocity spread. In recent years the complex stability criterion has been approximated as depending on the magnitude of  $Z$  divided by the frequency, and the coasting beam stability criterion has been applied to bunched beams. To improve on this less than satisfactory state of affairs computational work has been in progress for about a year to study a bunched beam, as reported by David Neuffer at this conference, and will continue, with the coupling impedance as a necessary input.

In all of the preceding no emphasis has been placed on the within bunch harmonics, either spatially or temporally. Such a harmonic analysis would be helpful if either the particles or the space charge waves executed many oscillations during the passage of the bunch through the accelerator. In the LIA case, a single particle on the average makes less than one synchrotron oscillation, while the space charge waves make at most two or three oscillations. The physical situation is better approximated by a middle portion, which is very much like a "coasting beam", and two bunch ends.

Feedback

The low speed of the ions and the long acceleration pulse duration make it possible to consider active feedback for longitudinal stabilization and waveform correction purposes. If the difference between an actual voltage and a desired voltage is detected and fed back to the beam, then the external impedance becomes zero. For such a scheme to be at all practical, as many known effects must be included in the voltage waveform as possible, so that only a small error signal has to be dealt with. Because of the low speed of the ions and the much lower intra-bunch velocities, the error signal could be accumulated over, for example, a 100 meter interval, and the correction applied further downstream. The most serious types of error are probably excessive tilts in energy, which could lead to premature bunching of the beam, and gross deficiencies in accelerating voltage such as might be caused by several misfires, which would tend to make the bunch slip out of its accelerating bucket. The correction for these types of errors would be a few cavities held in reserve, and triggered as required, to either change the average energy of the bunch or its variation along the bunch. The use of linear amplifiers would certainly work, but would be more expensive than the above method.



Applied, Beam Generated, and Total Electric Field and Bunch Current Waveforms

Figure 7